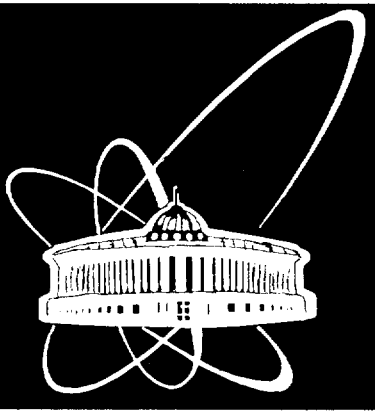

СООБЩЕНИЯ
ОБЪЕДИНЕННОГО
ИНСТИТУТА
ЯДЕРНЫХ
ИССЛЕДОВАНИЙ

Дубна

E9-2000-47

S.B.Vorojtsov, A.S.Vorozhtsov, F.Butin*, M.Price*

# ATLAS CAVERN MAGNETIC FIELD CALCULATIONS

*CERN, Geneva, Switzerland

31/33

2000

## Problem formulation

A review of the existing data on the map of magnetic field in the ATLAS cavern is timely because of modifications in the material and design of structural elements.

It should be noted that, at the moment, there is no complete field map in the cavern. In the previous treatment the effect of the various iron structure elements around the detector were treated in a simplified way by assuming constant magnetisation. In addition, studies were focused mainly on the perturbations caused inside the muon system. Some of the structural elements were treated either very approximately (e.g. the neutron shielding) or not considered at all (support trays for services of end-cap calorimeters and end-cap toroids). This was due either to the incomplete design at the time or by the poor justification of the constant magnetization assumption for the elements under consideration.

A new approach has been adopted to produce a complete ATLAS cavern B-field map using a more precise methodological approach (variable magnetisation, depending on the external field) and the latest design taking into account of the structural elements.

The following statements were made in Reference [1] and motivate the present study:

"Final calculations and/or measurements must be done when the final amount of ferromagnetic materials on the surrounding structure (racks, crates,...) becomes available".

"Further indicative values" should be mentioned there "for the region where power supplies and other ancillary electronics are located on the structure surrounding the ATLAS experiment".

"The deviations caused by the iron beams to the integrated field seen by the muon detector are small and in the range of one-tenth of a per cent in the vicinity of the surrounding structure.[2] This amount seems acceptable but must be taken into account in the final field calculations and measurements."

## Existing magnetic field data

In Reference [1] the existing magnetic field data have been outlined briefly.

### *Support and access structures. Magnetic impact analysis*

The magnetic impact simulations [3] concluded that the use of normal steel for construction was possible without disturbing the track reconstruction process beyond admissible limits.

A rough model of the HS was introduced in the general magnetic computations to assess its influence on the shape of the toroidal field in the region of the muon chambers. Note that the type of profile modelled was HE-900A. This represents a significantly larger quantity of material than has actually been retained for the design of the HS structure, thus overestimating the perturbative impact on the magnetic field.

The results of this analysis are given in Reference [3]. It is concluded that the proposed geometry of the surrounding structure, which involves significantly, less magnetic material than the geometry assumed in the magnetic calculations, has an

acceptable impact on the magnetic field in the muon spectrometer. Such a material is strongly preferred over stainless steel because of its lower cost.

### *Detector environmental conditions. Magnetic field*

The ATLAS detector includes four superconducting magnet systems: a central solenoid, two end-cap toroids, and the barrel toroid. The solenoid creates a 2 T field along the beam axis. The outer girder and the absorbers of the tile calorimeter form its return yoke. Indicative magnetic field values are given in Table 1.

**Table 1**

| Detector Component | B-field (Tesla) Lowest | B-field (Tesla) Average | B-field (Tesla) Highest |
|---|---|---|---|
| Inner tracker | 1.2 | 1.9 | 2.0 |
| EM Barrel | 0.1 | 0.2÷0.3 | 0.7 |
| Tile Barrel | 0.1 | 0.2÷0.3 | 0.5÷1 (girder) |
| Tile Extend. Barrel | 0.1 | 0.1 | 0.3 |
| Barrel/EB crack | 0. 2 | 0.4 | 0.6 |
| Barrel/EB gap | 0.01 | 0.04 | 0.08 |
| EM End-cap | 0.2 | 0.3÷0.4 | 0.7 |
| Had. End-cap | 0.01 | 0.3÷0.4 | 0.5 |
| Forward Calor. | 0.01 | 0.3÷0.4 | 0.5 |
| Radius 12m | 0.02 at z = 14.5m | 0.05 ÷ 0.07 at z = 12m | 0.05÷0.07 at z = 0m |
| Radius 14m | 0.01 at z = 14.5m | 0.02 at z = 12m | 0.02 at z = 0m |
| Radius 16m | 0.002 at z = 14.5m | 0.004 at z = 12m | 0.004 at z = 0m |

## Computer models

The dimensions of the cavern in the XOY plane (standard ATLAS system of coordinate, see Reference [1]) are given in Figure 1.

The final computer model of the cavern fields (with all the iron structural elements around the detector included) is complicated by a lack of symmetry simplifications. All of the 360°–azimuth range and ±Z half spaces must be taken into account. The ratio of the ferromagnetic element scale to be described within the model is very large: from the total cavern size (~ 30 x 29 x 53 $m^3$) down to the size of a pair of pliers.

However, the accuracy of calculations is defined by the impact of the field on the various electronic units, power supplies etc, and to the first order is not very high (~10%). Therefore, some simplifications in the description of the magnetic system of the detector are probably tolerable, since it is the external field that is under question.

The basic idea is to produce a dedicated basic TOSCA model and then to insert a series of ferromagnetic structure elements to monitor the perturbative effect on the basic field map.

One might also consider the Mermaid code [4],[5], to fit to the problem, on account of the huge number of nodes possible within Mermaid and its successful application for the development of various ATLAS magnetic field models. [6],[7]

The basic (i.e. with no additional iron insertion from the various structures around the detector) model of the stray field in the detector cavern is obtained by only considering the effect of the toroidal coils, the influence of the field from the solenoid–TileCal system is completely neglected. This assumption has been checked in the following section. The general conclusion is that the solenoidal part of the flux is pretty well localised within the TileCal iron and there is practically no field spreading to the muon system and beyond, into the cavern. The application of this model saves considerable computer time compared to the standard ATLAS model [8]. It takes just several minutes to get the results compared to hours for the standard model.

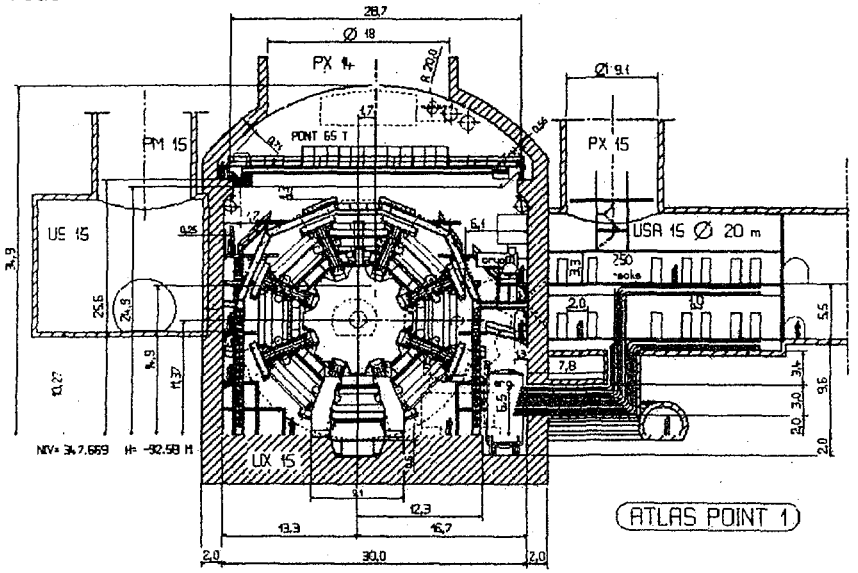


**Figure 1 Cavern cross section**

## Basic field map

The basic field map at various planes is presented in Figure 2 to Figure 10. In the captions of the Figures the term $B_{max}$ means that the field histogram is plotted in the range of $0 \div B_{max}$. The dashed lines represent an approximate contour of the cavern inner wall.

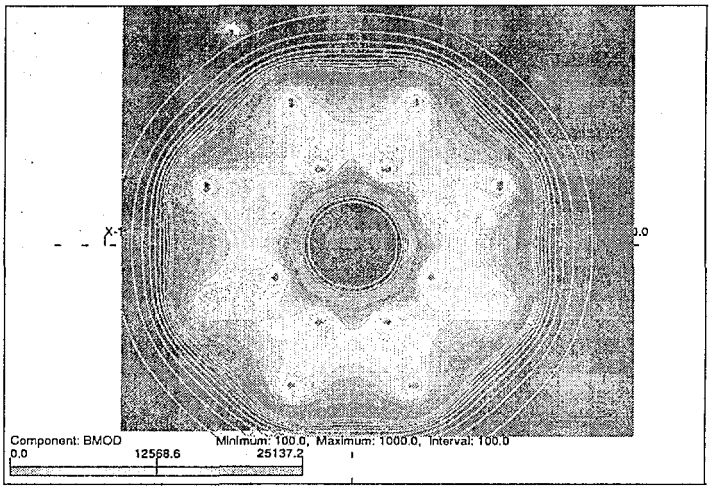


**Figure 2 XOY-plane**

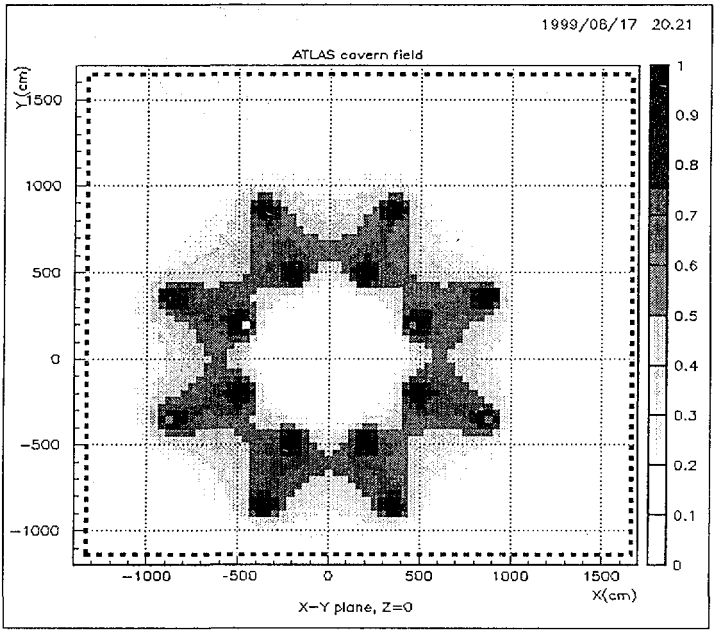


**Figure 3 XOY-plane, $B_{max}$ = 1 Tesla**

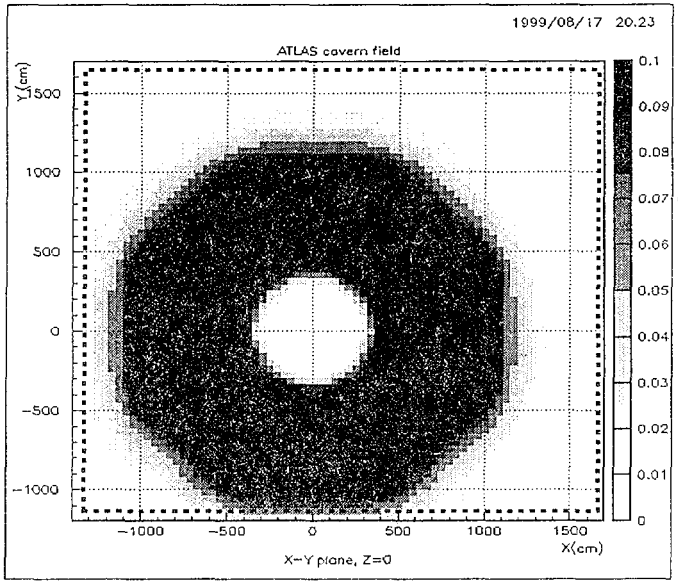


**Figure 4 XOY-plane. $B_{max}$ = 0.1 Tesla**

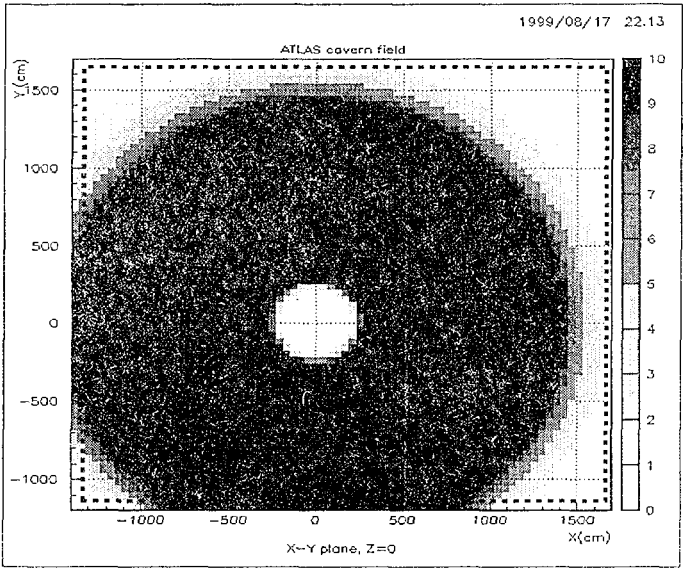


**Figure 5 XOY-plane, $B_{max}$=10 mT**

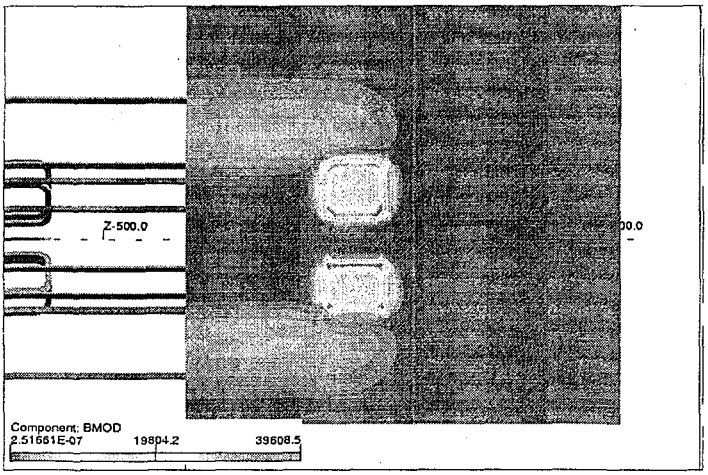


**Figure 6 R-Z plane, φ=0°**

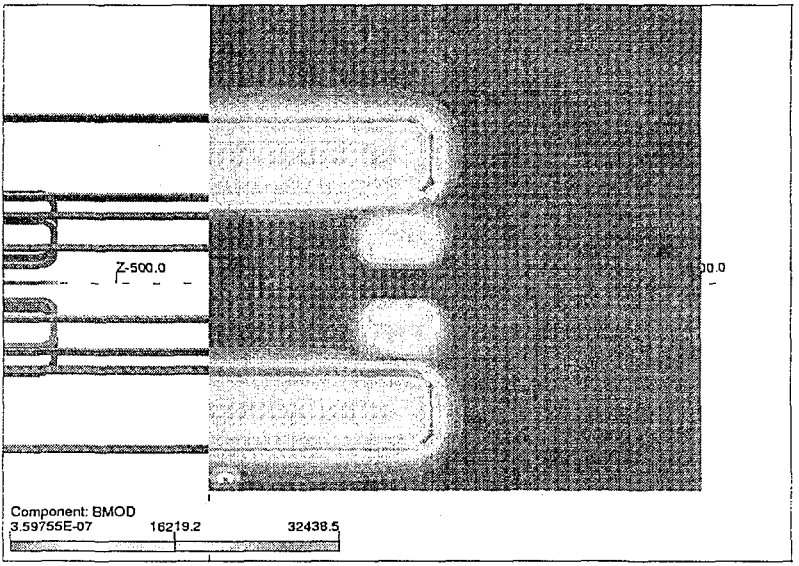


**Figure 7 R-Z plane, φ=22.5°**

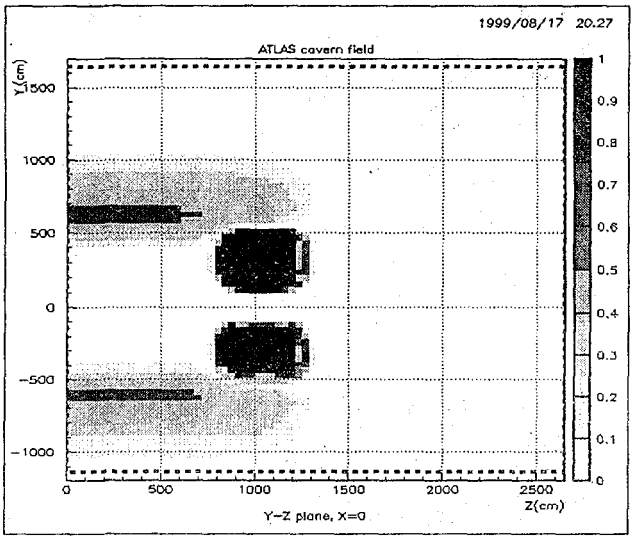


**Figure 8 YOZ-plane. $B_{max}$=1 Tesla**

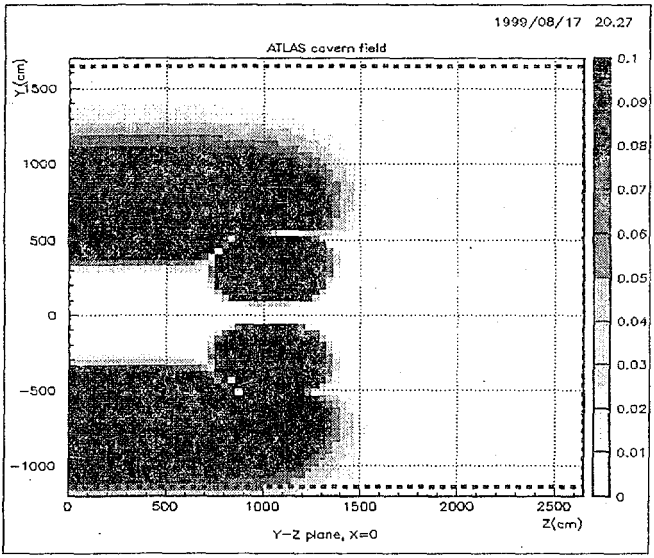


**Figure 9 YOZ-plane. $B_{max}$=0.1 Tesla**

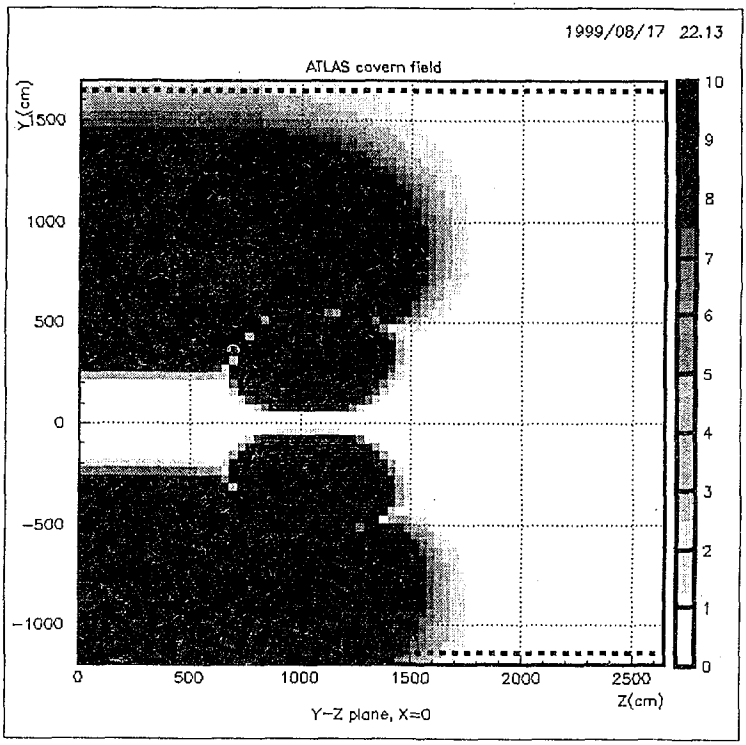


**Figure 10 YOZ-plane. $B_{max}$=10 mT**

## Comparison with existing ATLAS computer model

To check the validity of the model developed for the field map calculations outside the detector magnetic system, the present results have been compared with the existing standard ATLAS magnet computer model, Figure 11, Figure 12, Figure 13 and Figure 14. In these Figures one can see that the results of calculations are practically coincident. The maximum difference between two models is only of the order of ≈ 1 mT. This means that the model developed fully describes the external field and there is no need to insert the TileCal iron and solenoid. This drastically simplifies the problem of the full ATLAS magnet description. In addition, the present approach does not use any symmetry considerations. It is very important for the assessment of the field perturbation by the various iron insertions into the basic model.

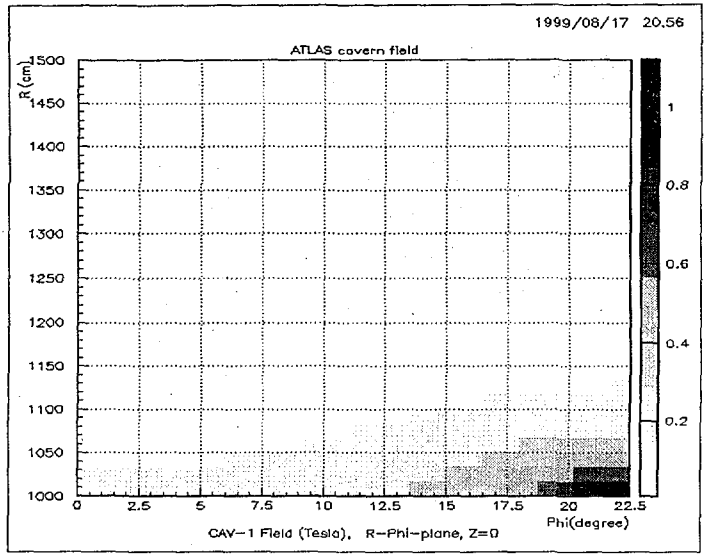


**Figure 11 R-φ surface field map, Z=0**

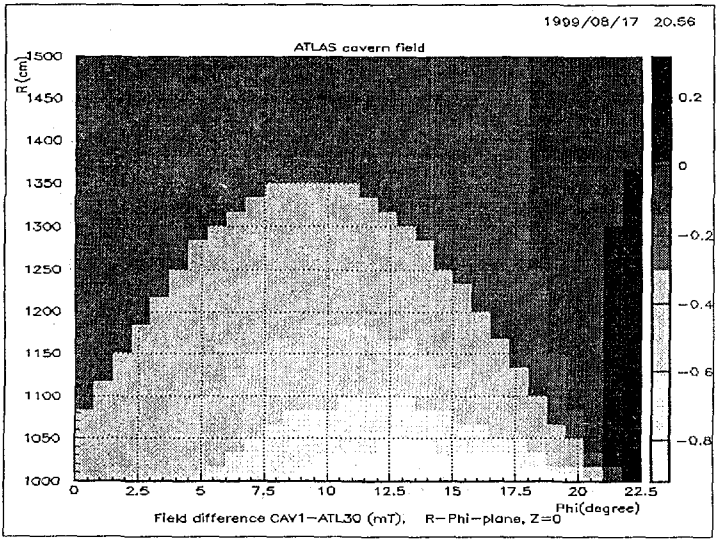


**Figure 12 Basic model error estimation at the R-φ surface, Z=0**

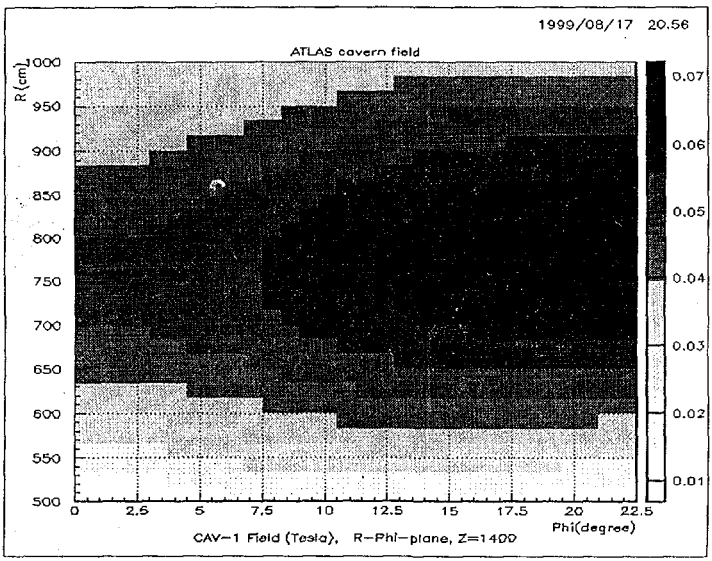


**Figure 13 R-φ surface field map, Z=1.4 m**

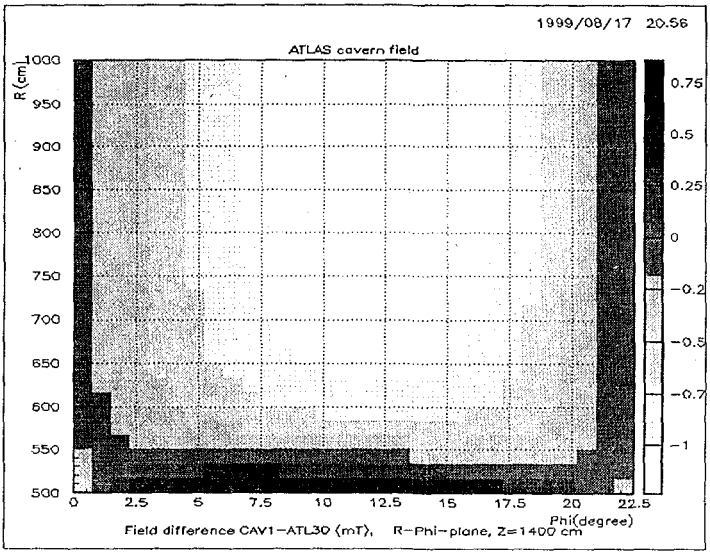


**Figure 14 Basic model error estimation at the R-φ surface, Z=1.4 m**

## Bedplates

The perturbative effect of the bedplates to the basic field map has been already estimated under the assumption of constant magnetisation of their material in the stray field of the toroid (see Reference [3]). In this note the variable magnetisation is taken into account. The evolution of the design (Figure 15) has also been taken into account in the computer model. A simplified form of the bedplate, with the maximum cross-section in the XOY plane, was considered in the calculations. No details of the bedplate's internal structure (windows etc) were taken into account. The bedplate was assumed to be a uniform box in the Z-axis cross-section and with a wall thickness of 40 mm. In this way an upper limit on the effects of the bedplates is obtained.

The results of the calculations show that the bedplate material is highly non-uniformly magnetised (Figure 16) with the maximum field at the saturation level $\approx$2.1 T (at the surface closest to the BT-coil). The parts of the bedplates nearest the toroid system are most highly magnetised. The end-effects are also quite visible. Nevertheless, the constant magnetisation approach at least gives an order of magnitude of the effect and is not a bad approximation for assessing the field perturbation in the vicinity of the bedplates.

A comparison of the field map around the bedplate and at the corresponding location without bedplates shows a considerable modification of the field pattern due to their presence (Figure 17). The detailed distribution of the field and the effect of the field perturbation are shown in Figure 18, Figure 19 and Figure 20. In these figures the position of the MDT chamber (sector 12) is depicted with a black contour to show the field distortion at its location. One can see that the field perturbation is an order of magnitude above the permissible level. This means that the bedplates should be made from nonmagnetic material or careful evaluation of their field should be considered in the event reconstruction codes. The conclusion agrees with the results of Reference [3].

Since normal steel is strongly preferred over stainless steel, because of its lower cost, detailed calculations of the magnetic field and/or magnetic measurements would be needed to assess the field perturbation by bedplate.

To complete the analysis of the bedplate effect the forces and torques, acting to the one half of one bedplate (x>0, z>0 zone), were estimated. The results are as following:

Fx $\approx$2 tonnes, Fy $\approx$ 18 tonnes, Fz $\approx$ –0.1 tonnes.
Coordinates of point of action for torque: x=y=z=0.
Tx $\approx$ –100 tonne·m, Ty $\approx$18 tonne ·m Tz $\approx$83 tonne ·m.

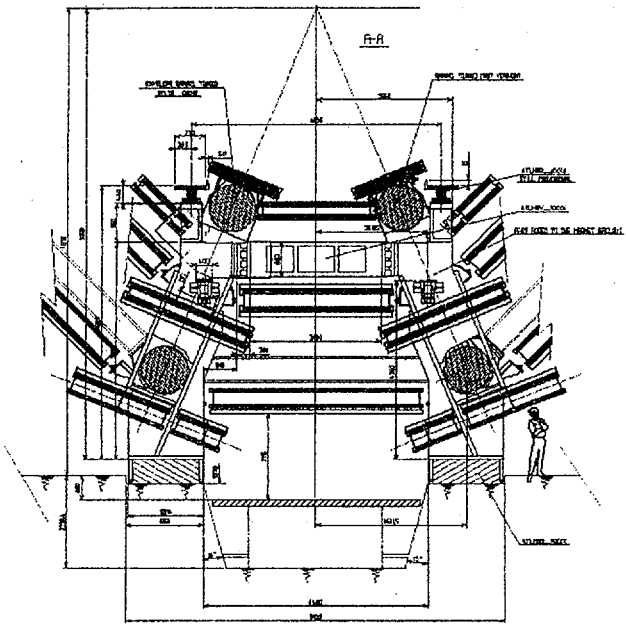


**Figure 15 Bedplate positions**

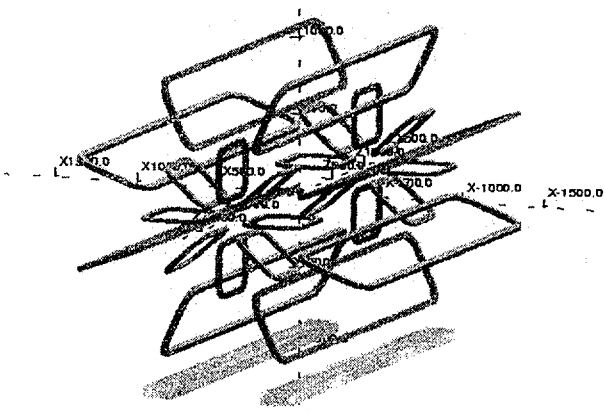


**Figure 16 Computer model**

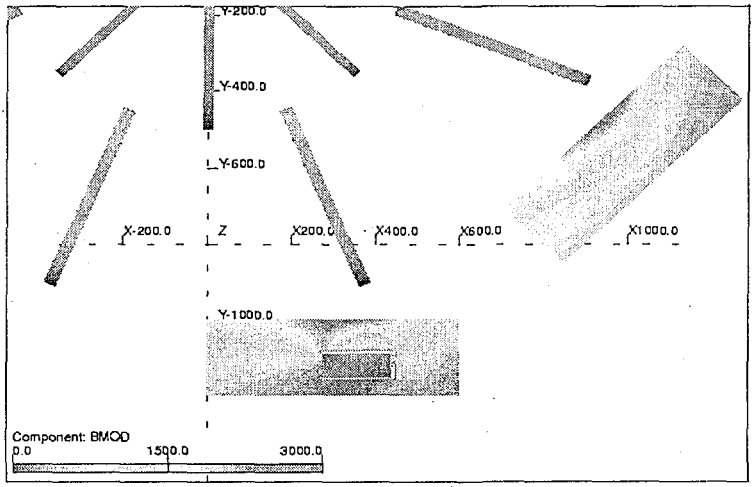


**Figure 17 Field map**

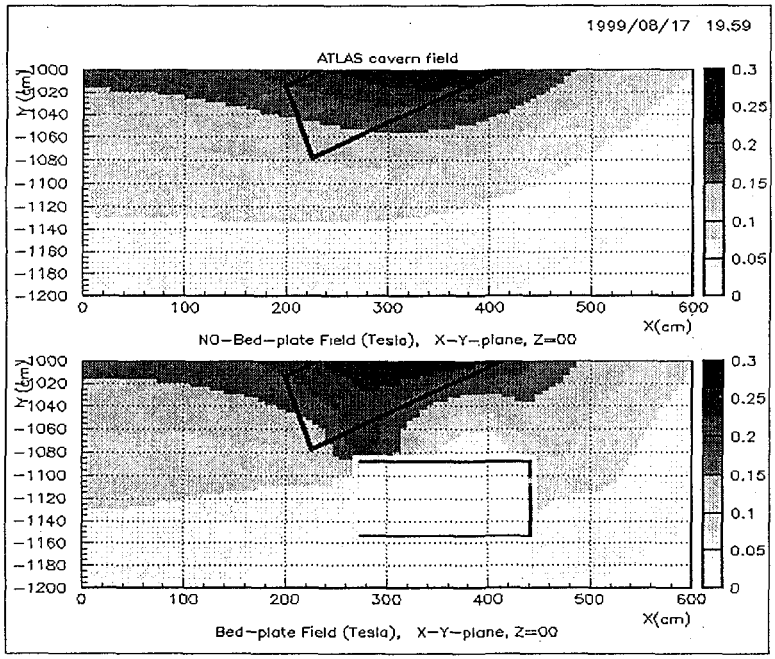


**Figure 18 Details of the field map**

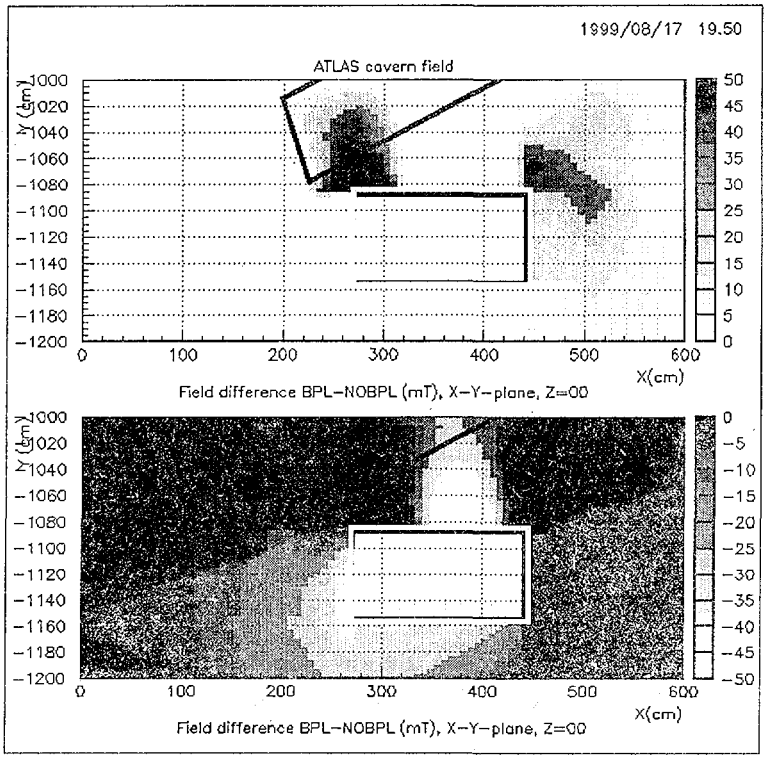


**Figure 19 Bedplate field contribution**

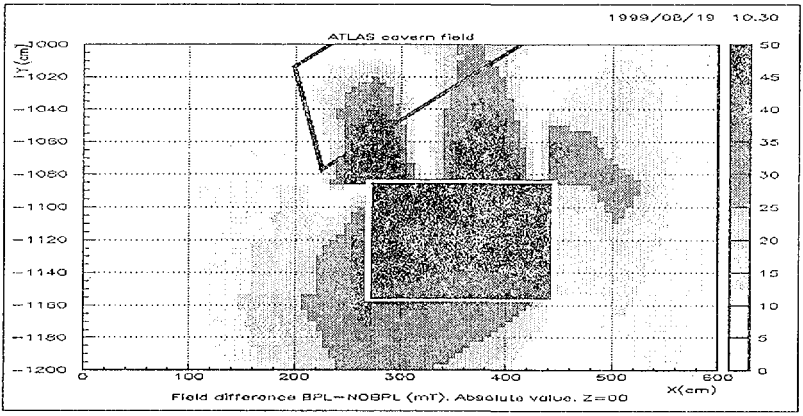


**Figure 20 Absolute value of the field distortion by bedplate**

## The cavern floor and bedplates

One should mention in connection with the results of the previous section that the cavern floor itself contains much ferromagnetic material. There could be a smoothing effect of the bedplate field perturbation due to the attraction of some part of the magnetic field flux to the cavern floor. To check all these considerations the cavern floor was introduced into the model with the packing factor = 1 to assess the maximum effect of the floor; i.e. it is assumed that the floor is made of ferromagnetic material.

In Figure 21 the corresponding field map in the region of interest is shown. The beplate and cavern floor (blue in the picture) with the trench in the bottom of the picture, near the X=0 plane, are recognisable in the Figure. One can see that there is no decrease of the bedplate perturbation due to the presence of the cavern floor in the model. It is clear from the Figure that the major part of the perturbation is connected with the proximity of the rectangular bedplates to the MDT chamber.

One might wish to pose a question: what would be the perturbation in the region of the MDT due to the cavern floor in the case where the bedplates are made of a non-magnetic material. To obtain a quantitative answer the floor packing factor should be known. We feel that the effect will still be less than for the bedplates, since the perturbing angle of the floor trench is far from the MDT region and the expected packing factor is less than 1.

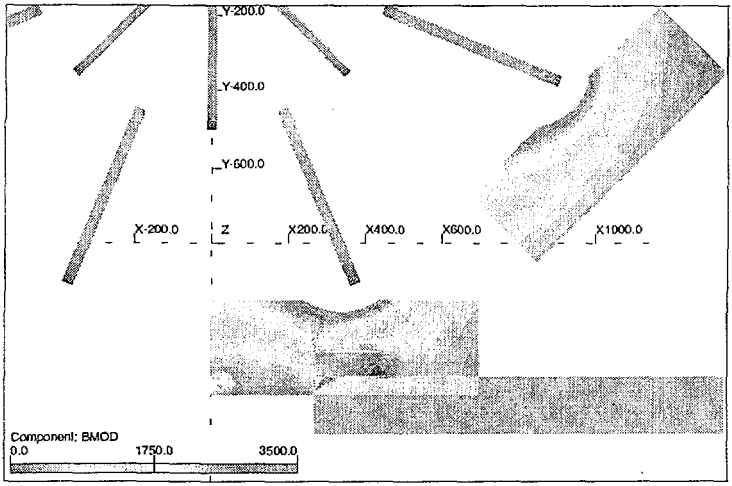


**Figure 21 Cavern floor effect**

## The surrounding support structure (HS)

The geometry of the surrounding structure is shown in Figure 22 (Reference [1]). The vertical posts support arches that span over the experiment. The vertical posts stand on the floor of the cavern and are connected to the cavern walls at mid-height. Cross bracing is added between the arches for reasons of longitudinal stability.

The surrounding structure (Figure 23) is split into six substructures. Each of these substructures is itself split into two main parts: the lower vertical posts, and the arches. The members of the HS make use of standard construction steel profiles (mainly HEA) with openings in the web through which services can be run.

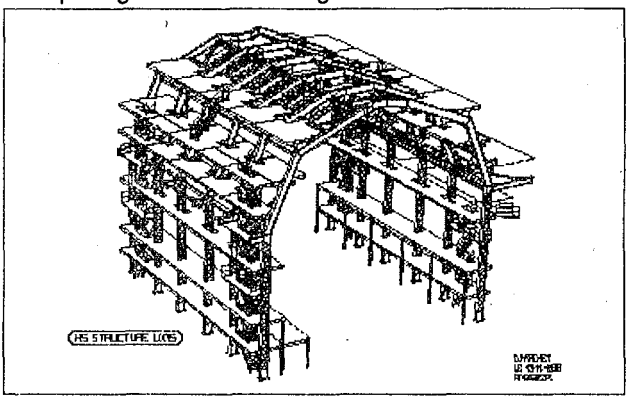


Figure 22 HS geometry

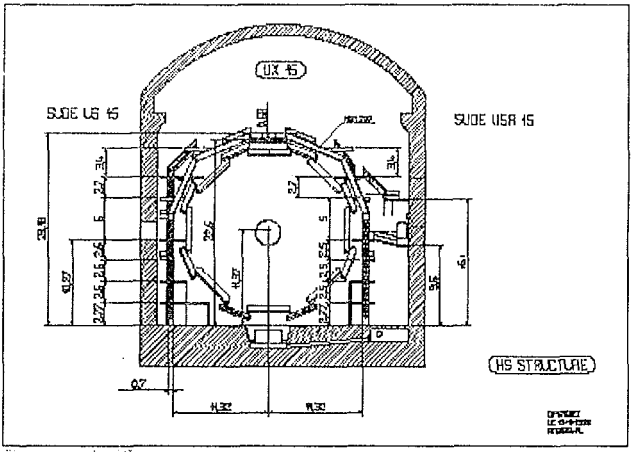


Figure 23 Main HS dimensions

## Racks

Racks can be positioned very close to the experiment and clearly be affected by the large stray fields present. This is particularly acute in the immediate vicinity of the muon system (Figure 24). The proposed racks in UX15 have dimensions of roughly 2355 x 600 x 950, with steel walls of 1 mm thick.

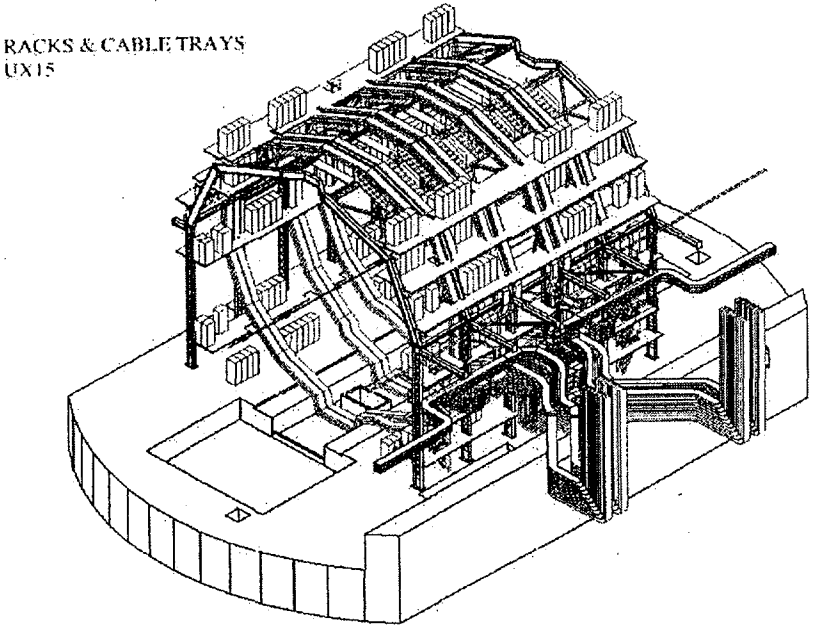


**Figure 24 Rack position in the UX15 cavern**

To assess the magnetic field distribution at the rack location the base field was calculated there (Figure 25 and Figure 26). This gives at least an order of magnitude of the real stray field. The field value at the rack position (≈ 150 mT) is higher than the permissible one (≈ 50 mT). Although the final position of racks is not fully defined at present there is little chance that ≈1mm thick steel box of racks would be able to screen the basic external field inside of the racks down to the permissible value. So, careful placement of the racks should be performed taking into account the detailed magnetic field distribution in the vicinity of the HS structure.

The final analysis of the magnetic field at the optimal rack locations should be done taking into account the contribution of the HS arches and the gratings. The shielding effect of the rack steel box at the given level of the external field could be also evaluated.

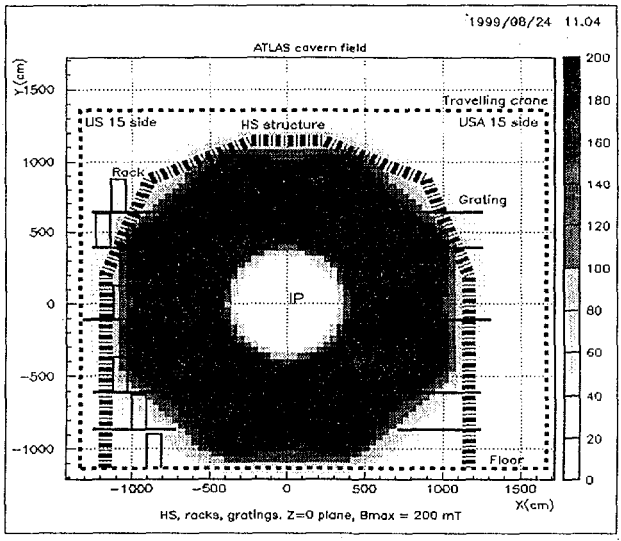


**Figure 25 Basic field map at the HS structure location**

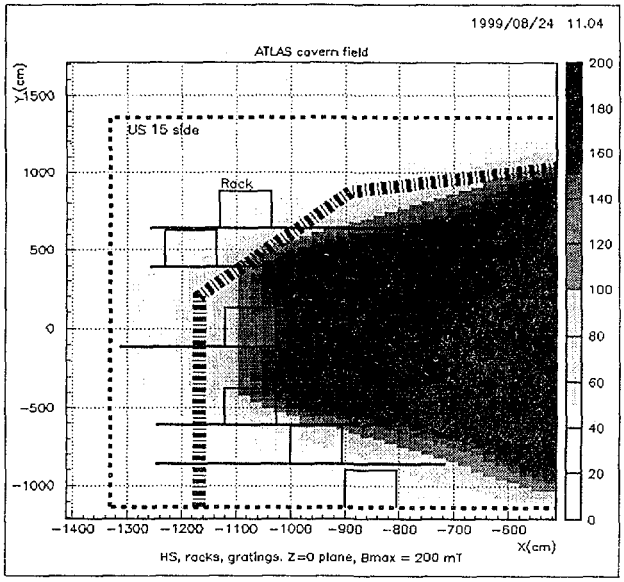


**Figure 26 Basic field map at the HS and rack location (US 15 side)**

## Conclusions

- The cavern basic field map was calculated.
- The bedplate field perturbation is an order of magnitude above the permissible level.
    - *Manufacturing of the bedplates from nonmagnetic material or careful evaluation of their field contribution in the event reconstruction codes is required.*
    - *Since normal steel is strongly preferred to stainless steel because of its lower cost detailed magnetic field calculations and/or magnetic measurement would be necessary to assess the field perturbation by the bedplates.*
- The cavern floor itself contains much ferromagnetic material and will also perturb the field at the location of interest.
- The field value at the rack positions is higher than the permissible one.
- The final position of racks should be chosen taking into account the detailed magnetic field distribution.

## References


[1] ATLAS Technical Coordination TDR, CERN/LHCC/99-01,ATLAS TDR 13, 31 January 1999.
[2] F. Bergsma, "Effects of an iron scaffolding on the toroidal field", private communication, 28/10/96.
[3] E. V. Samsonov, S.B. Vorojtsov, "Impact of some structure elements on ATLAS magnetic field", October 1997, EDMS: ATL-TC-EN-0021.
[4] MERMAID User 's Guide, Novosibirsk, 1994.
[5] MERMAID 2D & 3D for AT/386 Upgrade Kit. Novosibirsk, 1998.
[6] A.N.Dubrovin, S.B.Vorojtsov. "ATLAS Magnetic Field Calculation by Mermaid 3D Code". Internal report, BINP-JINR, October 1998.
[7] S.B. Vorojtsov, A.N.Dubrovin, M.Nessi. "3D Magnetic Field Calculations in the Finger Region of the TileCal" . Internal report, JINR-BINP-CERN, August 1999.
[8] F.Bergsma. "Calculation of average magnetic permeability of the ATLAS tile calorimeter." CERN/PPE-EC. April 1997.



Received by Publishing Department
on March 9, 2000.

## SUBJECT CATEGORIES OF THE JINR PUBLICATIONS

| Index | Subject |
|---|---|
| 1. | High energy experimental physics |
| 2. | High energy theoretical physics |
| 3. | Low energy experimental physics |
| 4. | Low energy theoretical physics |
| 5. | Mathematics |
| 6. | Nuclear spectroscopy and radiochemistry |
| 7. | Heavy ion physics |
| 8. | Cryogenics |
| 9. | Accelerators |
| 10. | Automatization of data processing |
| 11. | Computing mathematics and technique |
| 12. | Chemistry |
| 13. | Experimental techniques and methods |
| 14. | Solid state physics. Liquids |
| 15. | Experimental physics of nuclear reactions at low energies |
| 16. | Health physics. Shieldings |
| 17. | Theory of condensed matter |
| 18. | Applied researches |
| 19. | Biophysics |

Ворожцов С.Б. и др. E9-2000-47
Расчеты магнитного поля в зале эксперимента АТЛАС

Выработан новый подход при получении полной карты магнитного поля в пределах зала экспериментальной установки АТЛАС. При этом применялась более точная, чем ранее, методика расчета, учитывающая зависимость намагничивания структурных элементов от внешнего поля, а также последние проектные данные о структурных элементах.

Основная идея расчета заключалась в построении специальной расчетной модели детектора в рамках программы TOSCA с последующим включением в нее структурных ферромагнитных элементов для наблюдения эффектов возмущения базового поля детектора.

В конечном итоге было обнаружено, что возмущения поля от опорных элементов детектора на порядок превышают допустимый уровень. В связи с этим необходимо либо изготовление этих элементов из немагнитного материала, либо учет вклада поля от элементов в программах реконструкции.

Согласно расчетам значения поля в области расположения шкафов с электроникой также превышают допустимый уровень. Окончательное положение шкафов должно быть выбрано с учетом детальных расчетов распределения магнитного поля в этой зоне.

Работа выполнена в Лаборатории ядерных проблем ОИЯИ.
Сообщение Объединенного института ядерных исследований. Дубна, 2000

Vorojtsov S.B. et al. E9-2000-47
ATLAS Cavern Magnetic Field Calculations

A new approach has been adopted in an attempt to produce a complete ATLAS cavern B-field map using a more precise methodological approach (variable magnetisation, depending on the external field) and the latest design taking into account of the structural elements.

The basic idea was to produce a dedicated basic TOSCA model and then to insert a series of ferromagnetic structure elements to monitor the perturbative effect on the basic field map. Eventually, it was found:

The bedplate field pertubation is an order of magnitude above the permissible level. Manufacturing of the bedplates from nonmagnetic material or careful evaluation of their field contribution in the event reconstruction codes is required.

The field value at the rack positions is higher than the permissible one. The final position of racks should be chosen taking into account the detailed magnetic field distribution.

The investigation has been performed at the Laboratory of Nuclear Problems, JINR.

Communication of the Joint Institute for Nuclear Research. Dubna, 2000

Макет Т.Е.Попеко

Подписано в печать 11.04.2000
Формат 60 × 90/16. Офсетная печать. Уч.-изд. листов 2,07
Тираж 280. Заказ 51968. Цена 2 р. 50 к.

Издательский отдел Объединенного института ядерных исследований
Дубна Московской области